



An AARO Information Paper

Correlations of Starlink¹ Satellite Flaring with UAP Observations

December 2024

Introduction

With the advent of satellite communication mega-constellations including the SpaceX Starlink, Eutelsat OneWeb, Amazon Kuiper, and Chinese G60 constellations, there are currently thousands of artificial satellites in Low Earth Orbit (LEO)² and tens of thousands more planned for launch over the next decade [1]. Satellite flaring is an optical phenomenon which occurs when sunlight reflects off a satellite's surfaces, such as antennas or solar panels. This paper discusses specular and diffuse reflection of sunlight from man-made satellites and how these effects can be misinterpreted as unidentified anomalous phenomena (UAP). It also provides a method for observers to determine whether observations may be attributable to satellite flaring.

Background

Using reflected sunlight from man-made satellites to observe and track their movement goes back to the earliest days of space exploration [2]. As noted above, several companies develop and launch mega-constellations, providing internet access to most of the globe. Currently, there are nearly 10,000 artificial satellites in LEO and this number is expected to grow several-fold over the next decade [1]. Figure 1 illustrates the location of Starlink satellites in orbit as of December 2, 2024, at 11:00 AM Eastern Standard Time. As of the end of November 2024, there were over 6,700 Starlink satellites in orbit.

Figure 2 illustrates the concepts of diffuse and specular reflections, which describe how light bounces off objects. Figure 3 shows how sunlight reflected in these two ways is directed toward an observer on the surface of the Earth. As seen in the left side of Figure 2, diffuse reflection occurs when light reflects from a rough or irregular surface. Light impinging upon a rough surface reflects in many directions, which spreads the light over a large range of angles from the reflecting surface, as illustrated by the gray colored "light cone" in the Figure 3(a). From a single observation point, this cone of light can be visible for up to several minutes as the satellite moves in its orbit across the sky. Additionally, the intensity of reflected light significantly decreases the further away the observer is from the reflecting surface. At the Earth's surface, the intensity of diffusely reflected light from a satellite in LEO will typically have diminished to the point that the brightness is

¹ Any reference to a non-federal entity is for informational purposes only and does not constitute an express or implied endorsement of any commercial service, from AARO, the Department of Defense, or the Executive Branch. This report focuses on Starlink satellites, but its principles are applicable for any analogous satellite constellation.

² Altitude for Low Earth Orbit (LEO) ranges from 300km to 2,000km.

comparable to starlight. Due to their construction and orientation, many man-made satellites in LEO diffusely reflect sunlight and can appear as stars that move across the night sky.

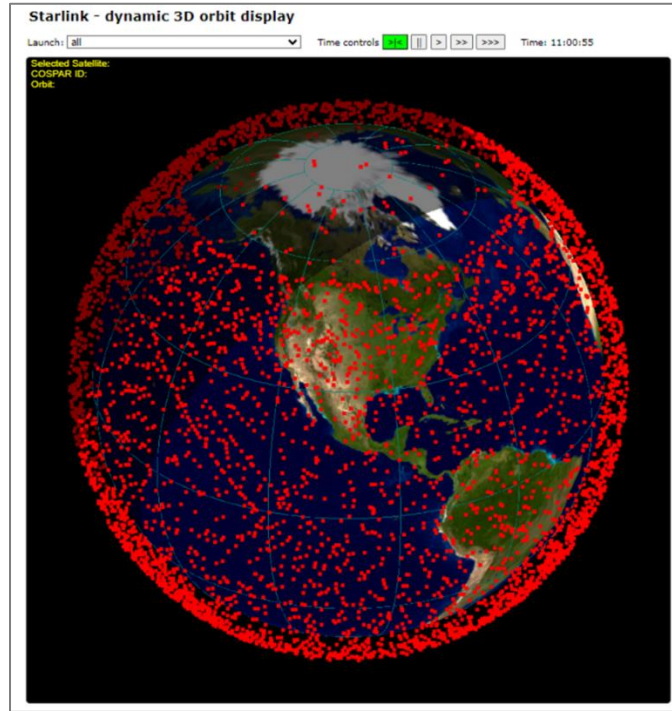


Figure 1: Graphic of Starlink satellites in orbit. Ref: <https://www.heavens-above.com/StarLink.aspx>

Specular reflection, also known as glint, occurs from a very smooth, mirror-like surface as illustrated on the right side of Figure 2. Unlike diffusely reflected light, the light striking a smooth surface reflects light at the same, or nearly the same, angle as the incident light. Therefore, the reflected light cone from a satellite in LEO is much narrower for specular reflection as compared to diffuse reflection, as illustrated in Figure 3(b). This dramatically increases its observed brightness by several orders of magnitude, but greatly decreases its observation time as the cone passes over the observer.

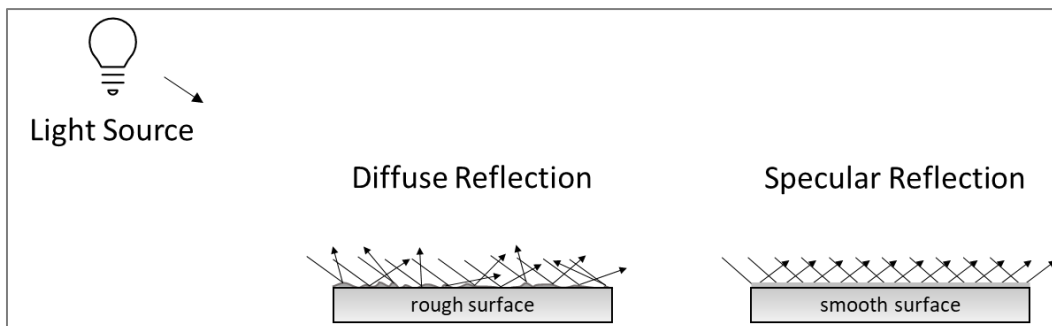


Figure 2: Image illustrating the difference between diffuse reflection (left) and specular reflection (right).

These very bright, short lived flashes of light are called “satellite flares” or “satellite glint.” The design, launch, and operation of SpaceX Starlink mega-constellations has led to a significant increase in the sighting of satellite flares, dubbed “Starlink flares,” noted by scientists and non-scientists alike.

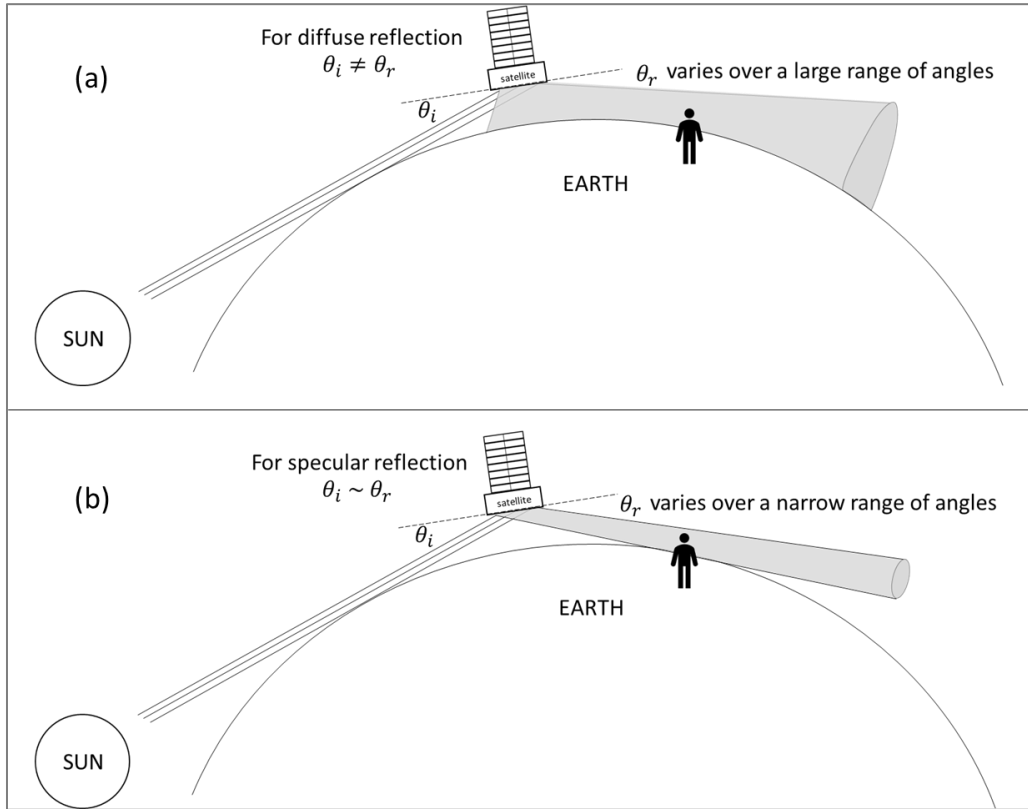


Figure 3: Illustration of (a) diffuse reflection of sunlight from a satellite and (b) specular reflection of sunlight from a satellite as viewed by an observer on the surface of the Earth.

Satellite Flares and Satellite Trains

Figure 4 shows a Starlink satellite in its operational configuration. Starlink satellites’ unique design and orientation make them susceptible to both diffuse and specular reflection, which causes their high visibility in the night sky. There are two key components to most satellites: (i) the solar panel, and (ii) the satellite bus. The solar panel provides a power source for the satellite bus. The bus is the primary body of the satellite that contains the electronics and systems to perform its designated mission. The Starlink bus has multiple mirrored panels and flat antenna arrays on the bottom side of the bus that faces the Earth in its operational configuration. Dependent on the generation of the Starlink satellite, the reverse side of the large solar panel can be a very efficient diffuse reflector, while the satellite bus is a very efficient specular reflector [3].

The phenomenon of satellite flaring is not new. This was well documented in the late 1990s and early 2000s after the launch of the Iridium satellite constellation [4]. However, satellite trains, or “Starlink trains,” are relatively new and result from the launch process SpaceX uses, which deploys

dozens of small satellites during a single launch event. Immediately following a launch, and for several days afterward, these satellites form a distinctive line of bright objects before fading as they ascend to their final orbital positions. Figure 5 below provides examples of each flare scenario.

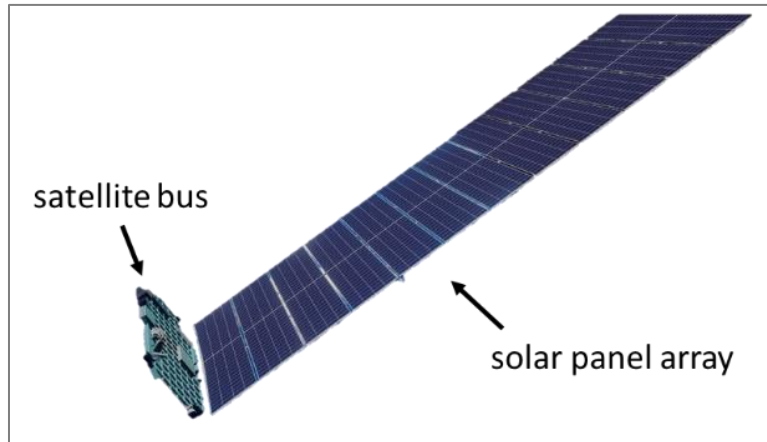


Figure 4: Rendering of Starlink satellite noting the satellite’s bus and solar panel components. Adapted from [5].

Starlink satellites transition through three orbital phases on their way to their final orbit, with each phase creating a different visual phenomenology to ground observers. During the launch phase, dozens of satellites, with their solar panels folded, are loaded in large groups on the rocket delivery vehicle. Once the delivery vehicle arrives to an initial position in LEO, the satellites separate and unfold their solar panels.



Figure 5: (a) photo of a string of Starlink satellites called “Starlink trains” not long after launch on 29 August 2022 [6]; and (b) photo taken by AARO personnel of a satellite flare at peak intensity for a Starlink satellite, which illustrates how much brighter Starlink flares can be than surrounding stars. Photo taken before sunrise on March 11, 2024 near Sidney, Nebraska. Camera settings: [7]

After the satellites have separated and traversed a specific distance from one another, they enter the second phase known as *orbital raise*. During this phase, the satellites navigate from their initial low orbit to their final orbital altitude, which is nominally 550km for the current generation of Starlink satellites. During the ascent, drag arises due to skin friction along the satellites' surfaces. To reduce the effects of drag, the satellites orient into a streamlined profile by shifting their solar panels parallel to the Earth, see Figure 6(a). It's this phase that creates the satellite trains, as light reflects off each solar panel of the ascending satellites. In the third phase, the satellites reach their final position called their *operational altitude*. Here the satellites reorient to their operational configuration with each satellite bus and its mirrored panels facing the ground and their solar panels extended above to maximize capture of sunlight.

It is this operational orientation of the satellites, Figure 6(b), that leads to flares or glint when the geometry of the Sun, satellite, and observer are properly aligned. These flares are orders of magnitude brighter than starlight and appear in a small section of sky called the "flare window." It is possible to have simultaneous flares from multiple satellites moving in differing orbits. To an observer on the ground, simultaneous flares might appear to be spinning lights, small glowing orbs that disappear and reappear, or tracing out geometric shapes such as triangles, or other odd morphologies that move quickly across this small section of the sky. To demonstrate how bright satellites can appear from the ground, AARO personnel photographed Starlink flaring on March 11, 2024, near Sidney, Nebraska (NE). These photographs are shown in Figure 7 and Figure 8. These images were taken using a 10 second exposure time which makes them appear as short streaks in the images versus point sources.

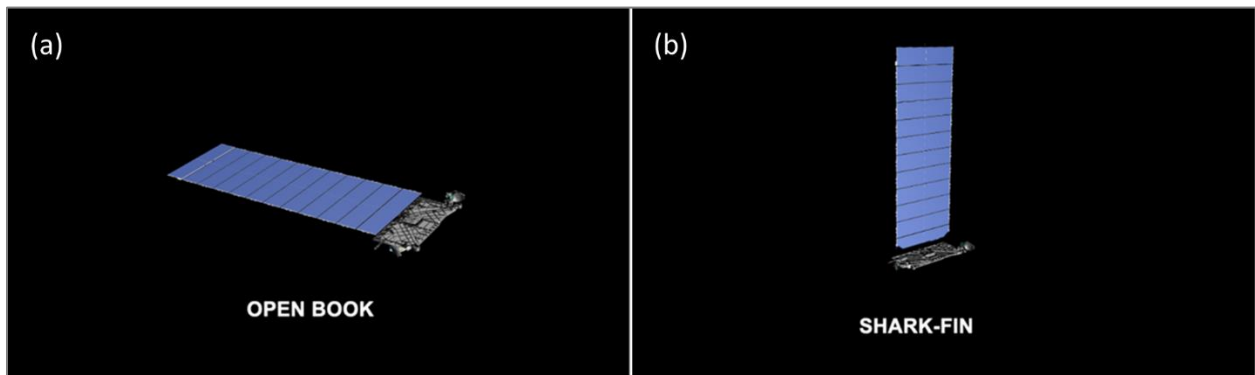


Figure 6: (a) rendering of Starlink satellite in its configuration during orbital raise; and (b) rendering of Starlink satellite in its final operational orbit. Adapted from [8].

Estimating When and Where to See Starlink Flares

The location and appearance of these flares is a function of the satellite's location, the Sun's position, the time, the date, and the observer's latitude. Many in the astronomy community are concerned about the light pollution created by satellite flares from these mega-constellations and their negative impact on scientific studies as well as the risks posed to the access and safety of space [9] [10] [11] [12]. This has driven some groups to create software models that predict the brightness of satellites based on their astronomical locations. Despite this, few publications exist

that discuss how to predict the azimuth and elevation angles of satellite flares to assist a ground-based observer. The key to performing this prediction is to understand the position of the sun relative to the satellite and the observer.

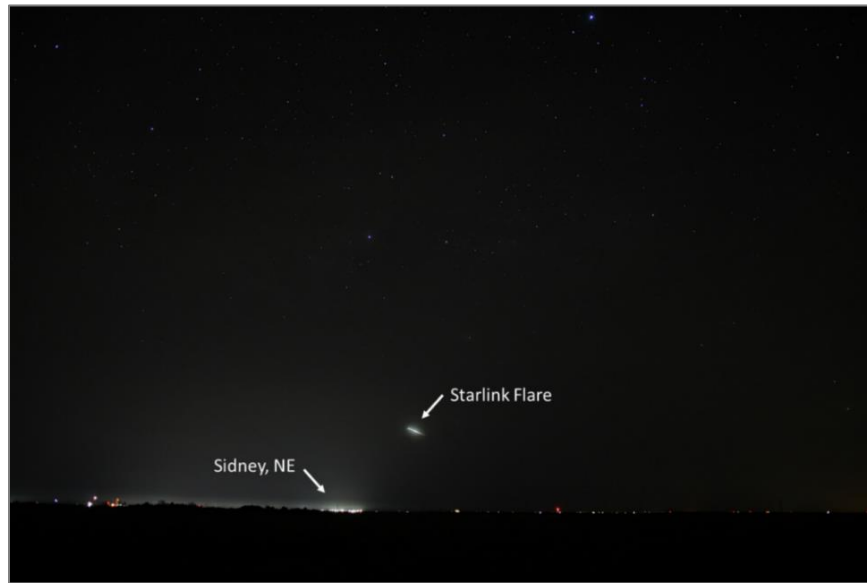


Figure 7: Image of Starlink flare taken by AARO personnel before sunrise on March 11, 2024 near Sidney, NE. Image was taken using a 10 second exposure time which led to the Starlink flare appearing as a streak instead of a point source. [7]

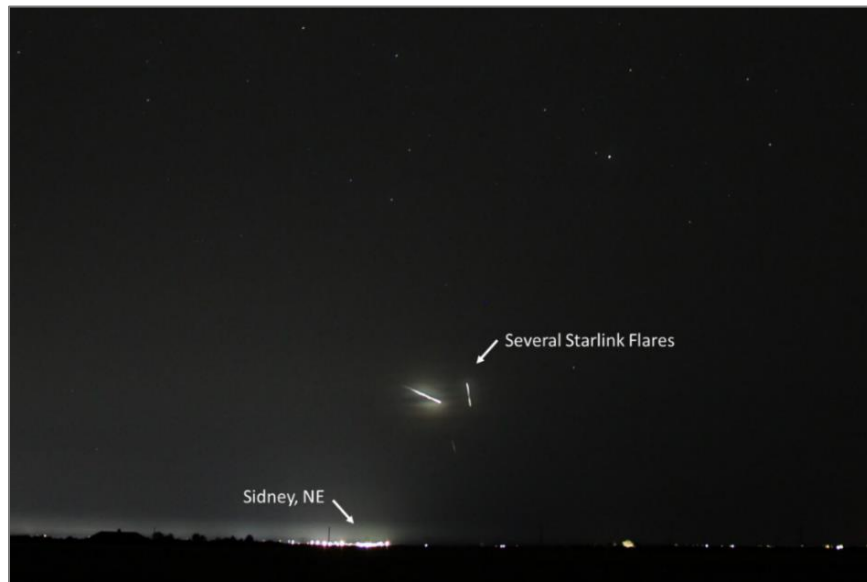


Figure 8: Image of multiple Starlink flares taken by AARO personnel before sunrise on March 11, 2024 near Sidney, NE. Image was taken using a 10 second exposure time which led to the Starlink flares appearing as streaks instead of point sources. [7]

The Sun's position in the sky can be described using two measurements: (i) the Sun's altitude angle, and (ii) the Sun's azimuth angle. The Sun's altitude, or solar altitude, is the angle between

the Sun and the Earth's surface at the horizon as viewed from an observer's position on the earth. During the day, solar altitude is a positive number expressed in degrees above the horizon. Solar altitude is negative at night, expressed in degrees below the horizon. Solar azimuth describes the angle to the Sun as referenced from true North at the observer's position, e.g., 90° being due East and 270° being due West. Seasonal changes affect the measurement of solar azimuth because of the Earth's 23.5° axial tilt. In the northern hemisphere, the Sun appears to rise and set further north each day between the winter and summer solstices. After the summer solstice, this cycle reverses, and the Sun rises and sets further south each day until the winter solstice. Thus, the specific azimuths of the rising and setting Sun are also dependent on the observer's latitude [13]. There are many online resources that will calculate the Sun's altitude and azimuth at a given time and date for a specific observer's location expressed in latitude and longitude [14] [15]. Similarly, the satellite's altitude with respect to an observer's position can be represented by an angle above the horizon. This look angle is the elevation angle from the horizon to the observation point in the sky, i.e., the point in the sky to potentially see flares. These geometries are shown in Figure 9.

The following calculations provide a guide to help observers predict when and where they might be able to view a satellite flare in the night sky. This is an *approximate* mathematical treatment and meant to be a guideline good to within a few degrees to help the observer estimate the look angles and times for Starlink flares.

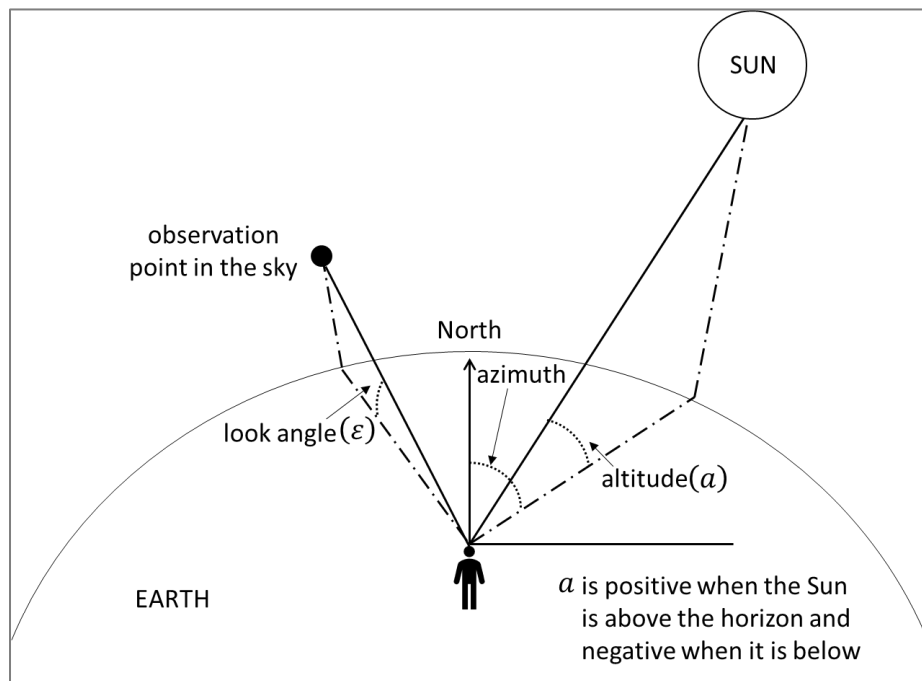


Figure 9: Cartoon of Sun's altitude and azimuth as referenced to the location of an observer on the Earth. Also defined is the look angle to observation point in the sky.

Using equations (11), (1) and (5) in reference [16], we can calculate the look angle to the satellite, ϵ , as a function of the Sun's altitude, a .

$$a(\epsilon) = \frac{\pi}{2} - \epsilon - \sin^{-1} \left(\frac{R_E}{R_E+h} \sin \left(\frac{\pi}{2} - \epsilon \right) \right) + \cos^{-1} \left(\frac{R_E}{R_E+h} \right), \quad (1)$$

where h is satellite height above the Earth's surface, R_E is the Earth's radius. As the zenith angle is complementary angle of the look angle, ε , the substitution $z = \frac{\pi}{2} - \varepsilon$ has been made in Equation (1).

Equation (1) is a transcendental equation, meaning that it must be solved numerically to find ε as a function of a , the sun's altitude. Using the mathematical software package MATLAB®, a plot was generated and is shown in Figure 10 for various Starlink satellite constellations, each of which have varying orbital altitudes between about 540km and 570km.

Figure 11 illustrates the geometry for a nominal Starlink orbital altitude of 550km. Simple trigonometry is used to determine that $\theta_r \cong \theta_i \cong 67^\circ$ and the angle $A \equiv |a| + \varepsilon \cong 46^\circ$. For perfect specular reflection and a satellite bus with its bottom surface that is aligned exactly perpendicular to its orbit, $A = 46^\circ$ and $\varepsilon = 0$. In other words, the satellite and resultant flare are directly at the horizon. Realistically, no surface is a perfect specular reflector and any small deviations from exactly perpendicular will reflect light off-axis resulting in $\varepsilon \neq 0$. Assuming the light cone is reflected as much as $\pm 2^\circ$ off axis, Starlink flares are then generally visible when the Sun's altitude is roughly between -38° and -46° as illustrated in Figure 10. This is determined from the inset in Figure 10, which shows that flares are visible somewhere between the horizon and about 10° above the horizon for up to 2° off axis reflection, as indicated by the dashed green lines.

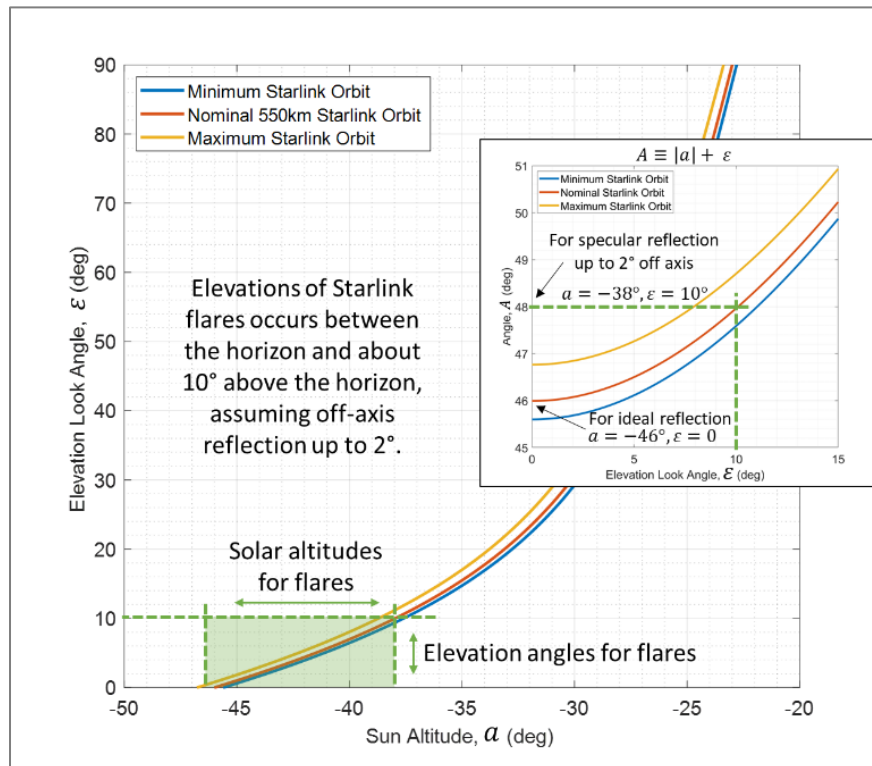


Figure 10: Plot of the Elevation Look Angle from the horizon to the satellite flare window as a function of the Sun's altitude below the horizon. Green lines indicate best set of Elevation Look Angles for observing Starlink flares is up to about 10° above the horizon assuming off-axis reflections up to 2° .

Error! Reference source not found. These numbers will vary for satellites with different orbital altitudes, but these guidelines are suitable for the current family of Starlink satellites.

Step-by-step Process to Estimate Location of Flare Window

We now have enough information needed to estimate the look angles to observe Starlink flares, specifically the sun’s elevation angle and satellite elevation angle. One can use the following process to predict the flare window’s azimuth and elevation. Table 1 provides a template for recording your observation.

Note the following information:

1. Choose the observation location (latitude and longitude).
2. Select the year.
3. Select the date.
4. Predict the Sun's azimuth at the chosen time, date, and location by entering the information from steps 1-3 into an online calculator of your choice. Two example calculators are <https://www.suncalc.org/> or <https://www.timeanddate.com/sun>.
5. Use the slider bar at the top of the page for suncalc.org or the expandable tables on timeanddate.com to find the time and azimuth after sunset when the Sun's altitude is -38° .
6. Record the Sun's azimuth and the local time of day.
7. After recording information from step 6, use the slider bar at the top of the page for suncalc.org or the expandable tables on timeanddate.com to find the time and azimuth after sunset when the Sun's altitude is -46° .
8. Record the Sun's azimuth and the local time.

Table 1: Example template for recording estimated azimuth and times for Starlink flare windows.

Observation Site		Latitude			NOTES:				
		Longitude							
After sunset					Before sunrise				
Date	Time (L)	Sun Altitude	Azimuth	Look Angle	Date	Time (L)	Sun Altitude	Azimuth	Look Angle
		-38°		10°			-46°		0°
		-46°		0°			-38°		10°
Measured Values of Satellite Flare					Measured Values of Satellite Flare				
Date	Time (L)		Flare Azimuth	Flare Elevation	Date	Time (L)		Flare Azimuth	Flare Elevation

9. Repeat steps 4 through 8 for the following day. Find the times and azimuths for the Sun before sunrise at -38° and -46° .
10. Using the information in the table, perform the observations and record the measured values in the table.

The scenario below illustrates this process by working through an example.

Scenario

Suppose AARO personnel want to gather images and video of Starlink flares to support the development of this information paper. AARO personnel travel from March 8-12, 2024, and select Sidney, NE as the destination. This is due to its ~4000 feet altitude within the High Plains and the generally flat terrain in this area, both of which make conditions more favorable to observe space-based objects near the horizon.

The necessary information is:

1. Observation location: Sidney, NE
2. Year: 2024
3. Day: March 10 after sunset and March 11 before sunrise

For steps 4 through 10, see Table 2 below. This was completed using <https://www.suncalc.org>. Table 2 shows that the measured azimuths and altitudes of the exemplified flares fall within the predicted values. Figure 12 and Figure 13 are example photos taken during the two timeframes noted in Table 2. AARO used <https://theskylive.com/planetarium> to reference the flare locations against the known positions of other celestial bodies, which are noted in the images.

Implications for Airborne Observation

Up to this point, the discussion has assumed the observer is located on the surface of the Earth. However, the phenomena of satellite trains and flares are also visible from aircraft. The angles, geometries, etc. may differ, but the fundamental principles are the same. For an airborne observer, the opportunity to see flares can persist longer when flying East to West after sunset in the direction of the Sun or West to East before sunrise in the direction of the Sun because they can stay in the flare light cone longer.

Table 2: Example table completed for the scenario described above.

Observation Site		Latitude	41.0064°		NOTES:				
Sidney, NE		Longitude	-103.1260°						
After sunset					Before sunrise				
Date	Time (L)	Sun Altitude	Azimuth	Look Angle	Date	Time (L)	Sun Altitude	Azimuth	Look Angle
03/10/24	10:22PM	-38°	305.2°	10°	03/11/24	2:44AM	-46°	38.1°	0°
	11:20PM	-46°	321.6°	0°		3:43AM	-38°	54.7°	10°
Measured Values of Satellite Flare					Measured Values of Satellite Flare				
Date	Time (L)		Flare Azimuth	Flare Elevation	Date	Time (L)		Flare Azimuth	Flare Elevation
03/10/24	10:38PM		309.6°	3.2°	03/11/24	3:13AM		47.4°	3.7°

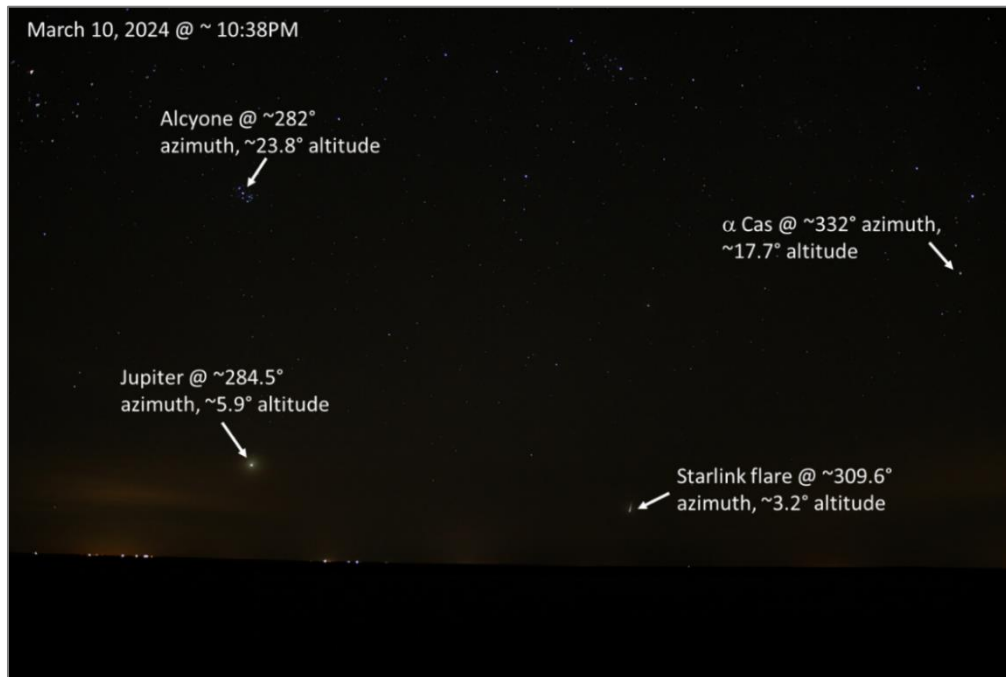


Figure 12: Images taken by AARO personnel near Sidney, NE after sunset on March 10, 2024. Note that the azimuth to the Starlink flares falls within the predicted angles in Table 2 at the time of image capture. Camera settings: [7].

Figure 14 shows the geometry of an airborne observer and two ground-based observers. The altitude of an airborne observer extends the Line-of-Sight (LOS) distance to the horizon as compared to a ground-based observer at the same latitude and longitude location, O_1 . For the airborne observer, this is equivalent to shifting their observation point by a distance d (the arc length) to align with a ground-based observer at position O_2 .

The LOS distance can be found using the Pythagorean theorem as:

$$R_{LOS} = \sqrt{(R_E + h_{ALT})^2 - R_E^2} \quad (2)$$

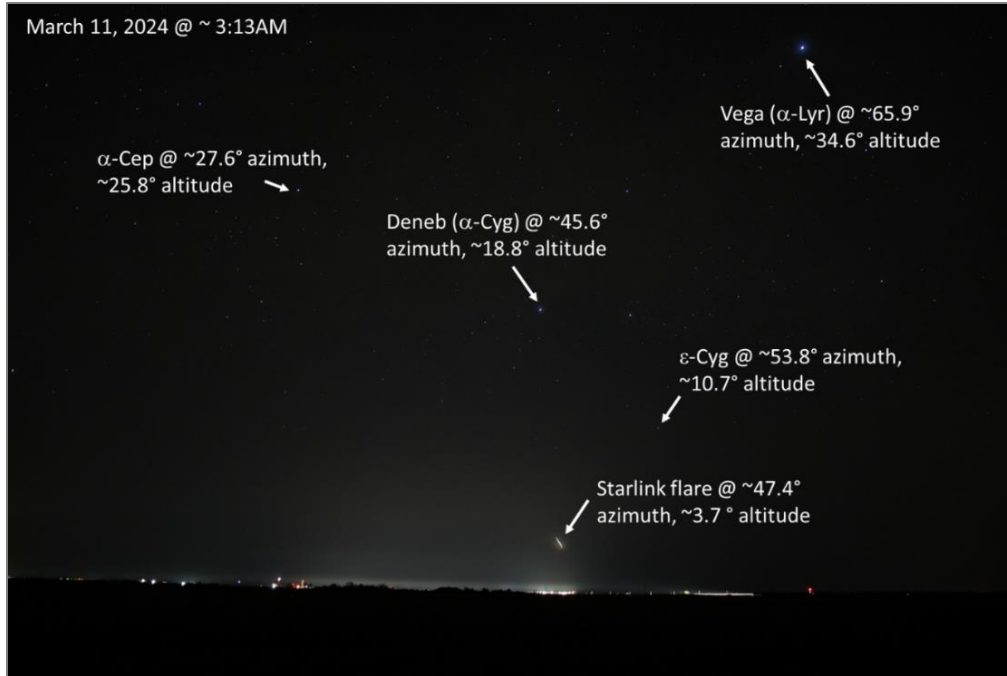


Figure 13: Images taken by AARO personnel near Sidney, NE before sunrise on 11-MAR 2024. Note that the azimuth to the Starlink flares falls within the predicted angles in Table 2 at the time of image capture. Camera settings: [7].

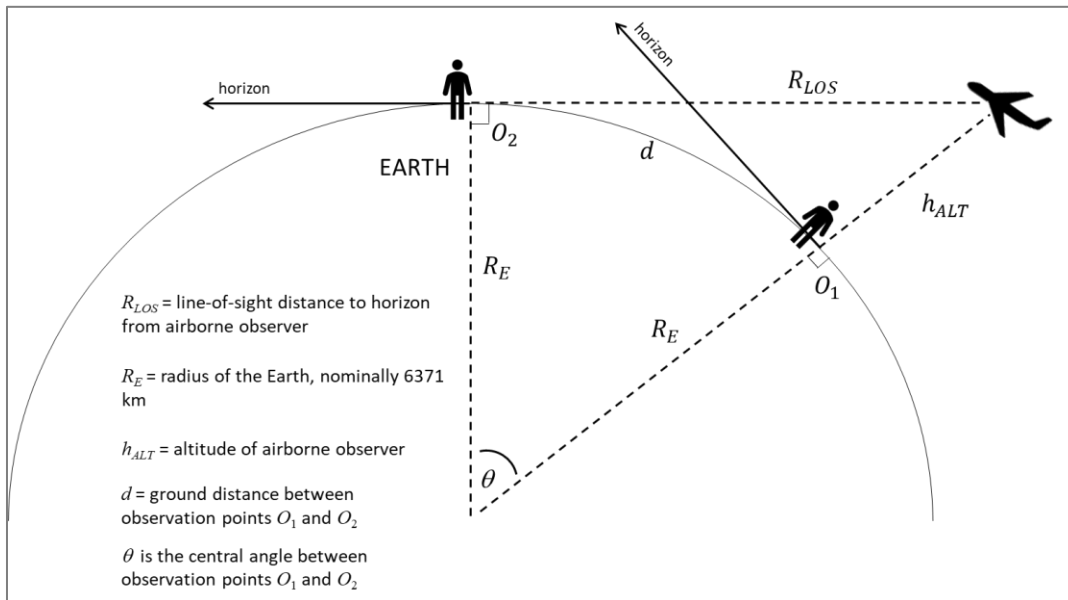


Figure 14: Diagram illustrating that an airborne observer at position O_1 , shares the same observation horizon as a ground-based observer at position O_2 . d is the projected shift of the observation horizon for the airborne observer.

which simplifies to:

$$R_{LOS} = \sqrt{2R_E h_{ALT} + h_{ALT}^2} . \quad (3)$$

Since $h_{ALT} \ll R_E$, then

$$d \approx R_{LOS} . \quad (4)$$

This relationship is plotted in Figure 15.

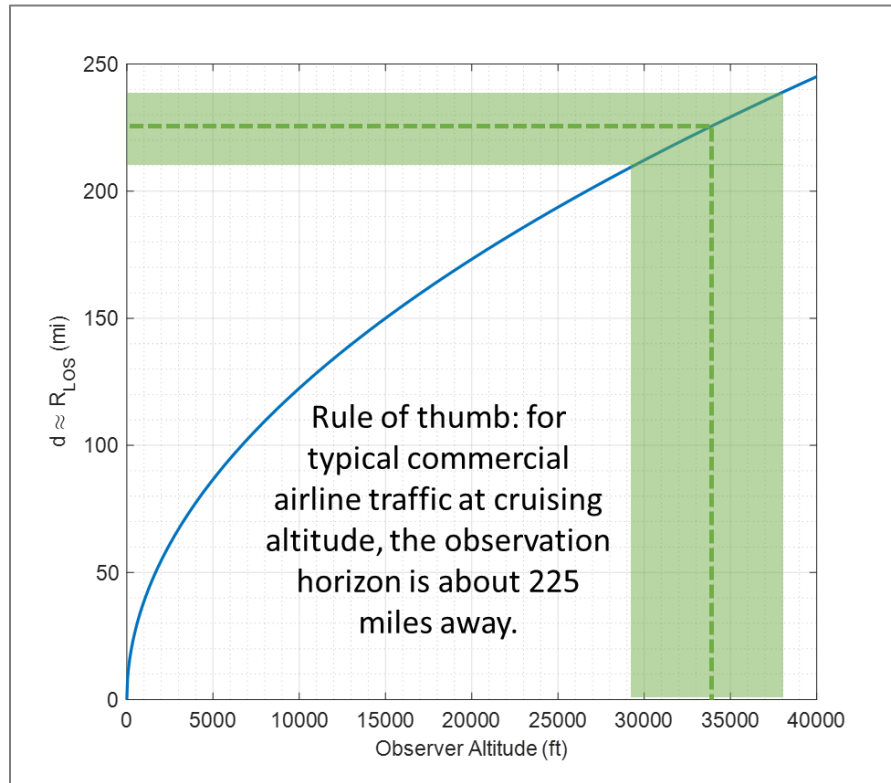


Figure 15: Projected shift in observation horizon (O_1 to O_2) as a function of observer altitude.

The latitude and longitude at position O_2 (the new effective observation point for the airborne observer) can be then estimated using the Haversine formula [17]. There are online calculators available to find the terminal coordinates when given a starting point, bearing and range, e.g., <https://www.fcc.gov/media/radio/find-terminal-coordinates>. Alternatively, one could use the ruler tool in Google Earth to estimate the terminal coordinates.

The coordinates for O_2 are used to determine the Sun's altitude and the observer's elevation look angle to potentially see flares for a given day, time, airborne observer location, and aircraft bearing (or azimuth look angle as noted in Footnote 3).

³ It is implied that the airborne observer is looking forward out of the aircraft cockpit, i.e., a pilot, thus, the aircraft bearing and azimuth look angle are approximately in the same direction. If the observer were a passenger looking out of a side window, then replace the aircraft bearing with the azimuth look angle of the observer as measured from true North to project O_1 to O_2 .

Unlike the ground-based observation case discussed above, an airborne observer does not have the ability to “park themselves” at a given location and wait for the Starlink flaring window to come into view. Consequently, the process described below is more likely useful to determine whether a previous sighting phenomenon may have been the result of Starlink flares.

Below is the process for determining the elevation and azimuth look angles for an airborne observer to determine whether their sighting may potentially have been due to Starlink flares. Table 3 is an example template that may be useful.

1. Choose the observation location (latitude and longitude, O_1), altitude and aircraft bearing for the airborne observer (or azimuth look angle as noted in Footnote 3).
2. Use Figure 15 and online resources or Google Earth to calculate the effective observation location, O_2 , for the airborne observer. Note the effective latitude and longitude in Table 3.
3. Select the year of the observation.
4. Select the calendar day of the observation.
5. Select the local time of the observation.
6. Determine the Sun's azimuth for the given time, date, and year at the effective observation position O_2 . If O_1 and O_2 are not in the same time zone, use the time zone for O_1 when converting from local time to UTC.
7. Go to the online Sun altitude and azimuth calculator of your choice, e.g., <https://www.suncalc.org/> or <https://www.timeanddate.com/sun/>, and enter the information from steps (2) through (5).
8. Use the slider bar at the top of the page for suncalc.org or the expandable tables on timeanddate.com to find the Sun's azimuth for the given local time of the observation and record this into the appropriate blocks in the table.
9. Use Figure 10 above to estimate the elevation look angle at which Starlink flares should have been visible and record this information into the table.
10. Compare the Sun's azimuth and elevation look angle for the estimated flare window to the sighting's azimuth and elevation to determine if Starlink flares may be a likely explanation for the observed phenomena.

Case

AARO received a Federal Aviation Administration UAP report from an airline pilot describing multiple unidentified lights moving in different directions. The report states that the pilot was traveling eastbound near Gallup, NM (35.5224°N, 108.7235°W) on October 9, 2022, at approximately 3:50AM local time. The aircraft was at an altitude of 35,000 feet and had a bearing (heading) of approx. 70° from true North. The pilot noted that the UAP were “multiple lights moving in different directions, left of the constellation Leo.” No further data was provided.

The following procedure will determine if the reported lights could be Starlink flares.

Table 3: Example template for recording estimated azimuth and elevation for Starlink flares that could explain the UAP sighting for an airborne observer.

Observation Site		Latitude, O ₁		
		Longitude, O ₁		
		Aircraft Altitude		
		Aircraft Bearing		
Effective Obs. Site		Latitude, O ₂		
		Longitude, O ₂		
Date	Time (L)	Sun Altitude	Sun Azimuth	Look Angle (Figure 10)
Sighting Parameters			Sighting Azimuth	Sighting Elevation

The necessary information is then:

- 1) Observation location, **O₁**: 35.5224°N, 108.7235°W
 Altitude: 35,000 feet
 Aircraft Bearing (also assumed to be observer's azimuth look angle): 70°
- 2) Using <https://www.fcc.gov/media/radio/find-terminal-coordinates>:
 The effective observation location, **O₂** is: 36.5987°N, 104.8259°W or near Cimarron, NM
- 3) Year: 2022
- 4) Date: October 9
- 5) Time: 3:50AM local

For steps 6 through 8, see completed Table 4 below. This was completed using <https://www.suncalc.org>.

Table 4: Example table completed for the airborne scenario described above.

Observation Site		Latitude, O ₁	35.5224°	
		Longitude, O ₁	-108.7235°	
		Aircraft Altitude	35,000 feet	
		Aircraft Bearing	70°	
Effective Obs. Site		Latitude, O ₂	36.5987°	
		Longitude, O ₂	-104.8259°	
Date	Time (L)	Sun Altitude	Sun Azimuth	Look Angle (Figure 10)
10/09/22	3:50AM	-38.5°	65.6°	~9° above the horizon
Sighting Parameters:			Sighting Azimuth	Sighting Elevation
			~63.3°	~5.7°

The specific azimuth and elevations of the sighting were not given, but the pilot does state that the UAP was to the “left of the constellation Leo.” Therefore, it is possible to approximate the sighting parameters by determining the Leo constellation’s location at the given day and time when viewed from the effective observation location, O_2 . Figure 16 below was generated using the planetarium view on the website https://in-the-sky.org/satmap_planetarium.php?. Noted in the image is information on several stars that provide a reference for estimating the sighting azimuth and elevation location “left of the constellation Leo.” Also shown are numerous Starlink satellites that were present in the sky during this time. The red satellites are estimated to be flaring per this website. The red arrows were added to the image by the author to show the direction of motion for several of the Starlink satellites. Note their crossing directions, which are consistent with the pilot’s report of “multiple lights moving in different directions.” The azimuth and elevation of the stars was determined using the website <https://theskylive.com/planetarium?>.

The estimated area of the sky the pilot likely referenced is circled by a white, dashed oval shape and the approximate center of this area is provided in the image. Using this estimate, it is possible to determine the sighting parameters required in Table 4. Comparing these to the expected location of the Starlink flare window for this date, time, and location (given by the Sun’s azimuth and look angle in the table), it is seen that these are very comparable. Consequently, the anomalous lights reported by the pilot are very likely Starlink and other satellite flares.

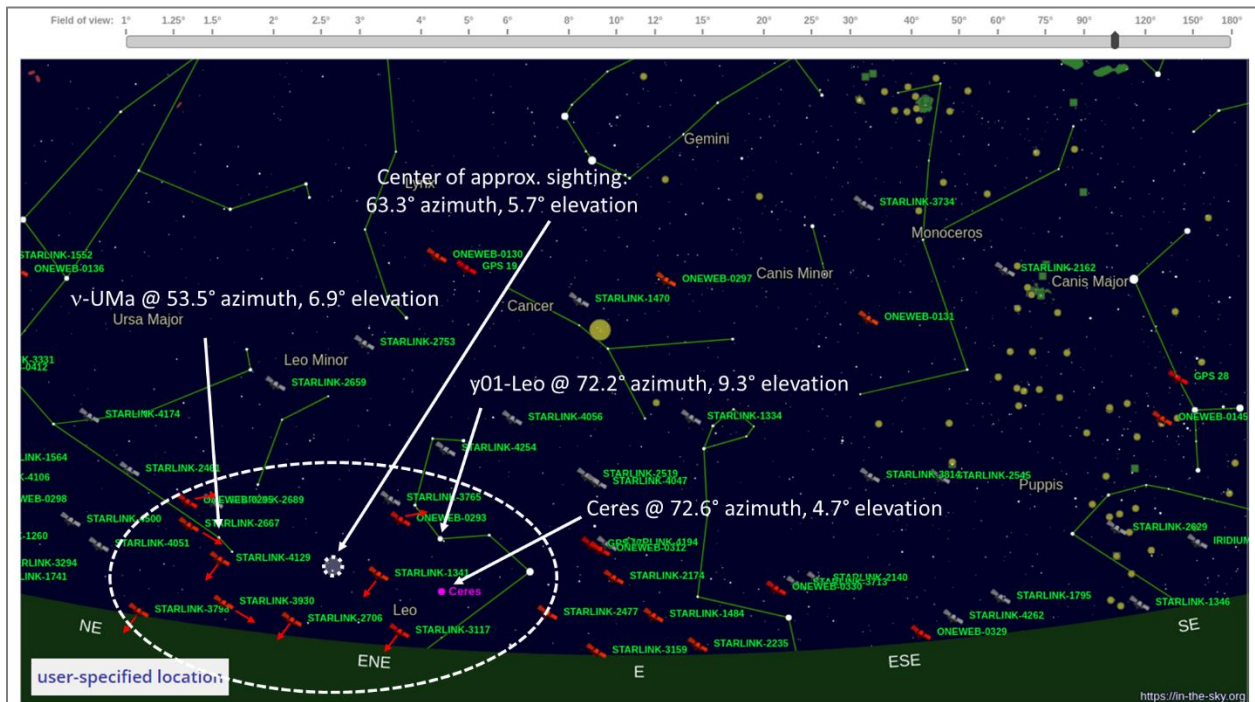


Figure 16: Graphic of predicted night sky as seen from an observer at location O_2 . Generated using reference [18].

Summary

Both diffuse and specular reflection of sunlight from satellites can explain some of the UAP reports received by AARO. Specular reflection from the mirrored panels and antennas on the satellite bus result in bright, short-lived flashes of light called “satellite flares.” Diffuse reflection from dozens of satellites launched in close spatial and temporal proximity by space-based communications companies, and particularly SpaceX, lead to “satellite trains.” These nighttime phenomena are the result of technological advances taken to proliferate global internet by placing thousands of satellites in LEO. This paper described these effects and provided references and processes, backed by examples, that can be used to predict or identify satellite flares. AARO anticipates that by equipping the reader with knowledge of this phenomena and the required information needed to deconflict satellite flares from UAP events, the quality of reports with supporting data and measurements will improve.

Acronyms

Acronym	Definition
AARO	All-domain Anomaly Resolution Office
LEO	Low Earth Orbit
LOS	Line of Sight
UAP	Unidentified Anomalous Phenomena

References

- [1] J. C. McDowell, "The Low Earth Orbit Satellite Population and Impacts of the SpaceX Starlink," *The Astrophysical Journal Letters*, p. L36, 2020.
- [2] R. Tousey, "VISIBILITY OF THE VANGUARD SATELLITE," in *NRL Participation in the CSAGI Rocket and Satellite Conference, September 30-October 5, 1957*, CA, OTS, U.S., Department of Commerce, 1959, p. 125.
- [3] SpaceX, "starlink.com," 2022. [Online]. Available: <https://api.starlink.com/public-files/BrightnessMitigationBestPracticesSatelliteOperators.pdf>.
- [4] N. D. James, "Iridium Satellites Light Up The Sky," *Journal of the British Astronomical Association*, vol. 108, no. 4, pp. 187-188, 1998.
- [5] "Sky News," 1 12 2022. [Online]. Available: <https://news.sky.com/story/starlink-elon-musks-satellites-to-beam-high-speed-broadband-to-remote-areas-of-uk-in-government-trial-12759097>.
- [6] J. Hsu, "New Scientist," 4 10 2023. [Online]. Available: <https://www.newscientist.com/article/2394949-starlink-carbon-footprint-up-to-30-times-size-of-land-based-internet/>.

- [7] AARO, "Canon EOS Rebel T7 f/1.8 10.0 sec exposure, ISO-800, 18mm focal length, no flash, compulsory, Sigma Lens 210-101, manual focus, auto white balance.," 2023.
- [8] M. Boucher, "Space Ref," [Online]. Available: <https://spaceref.com/science-and-exploration/spacex-publishes-update-on-starlink-satellite-brightness-issue/>.
- [9] J. C. McDowell, "The low earth orbit satellite population and impacts of the SpaceX Starlink constellation," *The Astrophysical Journal Letters*, vol. 892, no. 2, p. L36, 2020.
- [10] S. M. B. A. C. & R. H. Lawler, "Visibility predictions for near-future satellite megaconstellations: latitudes near 50 will experience the worst light pollution," *The Astronomical Journal*, vol. 163, no. 1, p. 21, 2021.
- [11] A. C. & B. M. Boley, "Satellite mega-constellations create risks in Low Earth Orbit, the atmosphere and on Earth," *Scientific Reports (Nature)*, vol. 11, no. 1, pp. 1-8, 2021.
- [12] J. e. a. Zhang, "LEO mega constellations: review of development, impact, surveillance, and governance," *Space: Science & Technology*, pp. 1-17, 2022.
- [13] NOAA Global Monitoring Division, [Online]. Available: <https://gml.noaa.gov/grad/solcalc/solareqns.PDF>.
- [14] T. Hoffmann, "SunCalc.org," [Online]. Available: <https://www.suncalc.org/>.
- [15] "Sunrise and Sunset Calculator," [Online]. Available: <https://www.timeanddate.com/sun>.
- [16] O. R. & W. A. P. Hainaut, "Impact of satellite constellations on astronomical observations with ESO telescopes in the visible and infrared domains," *Astronomy & Astrophysics*, vol. 636, p. A121, 2020.
- [17] "Kansas State University," [Online]. Available: <https://www.math.ksu.edu/~dbski/writings/haversine.pdf>.
- [18] "In The Sky," [Online]. Available: https://in-the-sky.org/satmap_planetarium.php?.
- [19] O. S. o. America, "Snell's Law, Reflection, and Refraction," 2008. [Online]. Available: <https://osa.magnet.fsu.edu/tutorials/snell.html>.